Ultrasound in Medicine & Biology 000 (2025) 1–10

Contents lists available at ScienceDirect

Ultrasound in Medicine & Biology

journal homepage: www.elsevier.com/locate/ultrasmedbio

Original Contribution

Response of Serum-Isolated Extracellular Vesicles to Focused Ultrasound-Mediated Blood-Brain Barrier Opening

Alina R. Kline-Schoder [a,$], Fotios N. Tsitsos [a,$], Alec J. Batts [a], Melody R. DiBenedetto [a], Keyu Liu [a], Sua Bae [a], Elisa E. Konofagou [a,b,c,*]

[a] Department of Biomedical Engineering, Columbia University, New York, NY, USA
[b] Department of Radiology, Columbia University, New York, NY, USA
[c] Department of Neurological Surgery, Columbia University, New York, NY, USA

ARTICLE INFO

Keywords:
Focused ultrasound
Blood-brain barrier
Extracellular vesicles
Immunotherapy
Biomarkers
Liquid biopsy

ABSTRACT

Objective: To characterize the response of extracellular vesicles (EV) in the serum of mice and Alzheimer's disease (AD) patients following focused ultrasound (FUS)-mediated blood-brain barrier (BBB) opening (FUS-BBBO) as a means to improve liquid biopsy.

Methods: Blood was collected from C57BL/6 mice before, and one hour after FUS-BBBO, and from AD patients before, one hour after, and three days after FUS-BBBO. EVs were isolated from serum using the Exoquick precipitation solution and their concentration was quantified using nanoparticle tracking analysis. The transcriptomic and proteomic content of EVs from mice was assessed using RNA sequencing and mass spectrometry protein analysis respectively. Additionally, the release of EVs in mice was inhibited using the GW4869 drug to assess the role of EVs in the restoration of the BBB. Finally, the biomarker content of EVs in AD patients was detected using a Luminex multiplex assay.

Results: We observed a 164±85% (95% confidence interval: 78.998 − 249.202) increase in murine EV concentration one hour after treatment, as well as an increase in EV RNA associated with FUS-BBBO neuroimmunotherapy. Inhibition of EVs reduced the inflammatory response and BBBO volume in mice. Patient EV concentration also increased one hour after treatment and was dependent on the volume of BBB opening three days post-treatment. Furthermore, EV isolation was found to significantly enhance ($p<0.05$) the detection of FUS-BBBO-induced amplification of AD and CNS biomarkers such as GFAP, beta-amyloid 42 and phosphorylated tau 181, exhibiting on average a 1.2 times higher log-fold change in biomarker levels in isolated EVs compared to total serum.

Conclusion: Overall, we hereby present the first evidence of altered murine and AD patient EV concentration and content in response to FUS-BBBO, providing evidence of EVs' role within FUS-BBBO neuroimmunotherapy as well as their utility in improving FUS-BBBO biomarker amplification. Our results pave the way for clinical applications of EV-based liquid biopsy in patients with neurodegenerative diseases following FUS-BBBO, as a way of noninvasively monitoring disease progression.

Introduction

The blood-brain barrier (BBB) is a virtually impermeable barrier between the blood and the brain that keeps the brain at homeostasis for neuronal firing. In addition to limiting the infiltration of neurotoxins and pathogens, the BBB limits both the delivery of drugs to the brain and the circulation of neurological disease biomarkers in the blood [1]. Focused ultrasound-mediated blood-brain barrier opening (FUS-BBBO) combines focused ultrasound with intravenously administered microbubbles to transiently and noninvasively open the BBB, tackling these two challenges [2–4].

Abbreviations: AD, alzheimer's disease; BBB, blood-brain barrier; cfDNA, cell-free DNA; CNS, central nervous system; EV, extracellular vesicle; FUS, focused ultrasound; FUS-BBBO, focused ultrasound-mediated blood-brain barrier opening; GFAP, Glial fibrillary acidic protein; HRP, horseradish peroxidase; LC/MS ESI-TOF, liquid chromatography/mass spectrometry electrospray ionization time-of-flight; LogFC, log fold change; MB, Microbubble; miRNA, micro-RNA; MRI, magnetic resonance imaging; ncRNA, noncoding RNA; NTA, nanoparticle tracking analysis; PBS, phosphate-buffered saline; piRNA, piwi-interacting RNA

* Corresponding author. Elisa E. Konofagou, Department of Biomedical Engineering, 351 Engineering Terrace, Mail Code 89041210, Amsterdam Avenue, New York, NY 10027, USA.
E-mail address: ek2191@columbia.edu (E.E. Konofagou).
$ These authors contributed equally.

https://doi.org/10.1016/j.ultrasmedbio.2025.04.019
Received 4 February 2025; Revised 25 April 2025; Accepted 28 April 2025

Please cite this article as: A.R. Kline-Schoder et al., Response of Serum-Isolated Extracellular Vesicles to Focused Ultrasound-Mediated Blood-Brain Barrier Opening, Ultrasound in Medicine & Biology (2025), https://doi.org/10.1016/j.ultrasmedbio.2025.04.019

Although initially designed to facilitate drug delivery through the BBB, FUS-BBBO has also been established as a neuroimmunotherapeutic treatment for neurological diseases and a method of amplifying the detection of neurological biomarkers [4–10]. As a neuroimmunotherapeutic, FUS-BBBO has been shown to reduce disease pathology and ameliorate disease-associated cognitive deficits in many neurological models ranging from Alzheimer's Disease (AD) to depression [6,11]. These effects coincide with brain macrophage modulation, increased neurogenesis, and increased synaptic plasticity [5,12,13]. FUS-BBBO amplification of neurological biomarkers has been primarily investigated in models of brain cancer, where reports have found increases in circulating cell-free DNA (cfDNA), as well as central nervous system (CNS) proteins, including Glial Fibrillary Acidic Protein (GFAP), in response to treatment [4,7–10].

Extracellular vesicles (EVs) are lipid vesicles responsible for cell transport and exchange. EVs have a highly variable cargo, including proteins, carbohydrates, and/or coding and noncoding RNA (ncRNA). Due to their small size, there is a particular emphasis on ncRNA within EVs such as micro RNA (miRNA) and piwi-interacting RNA (piRNA). Both miRNA and piRNA regulate the mRNA transcription of target protein-encoding genes. There are publicly available databases of miRNA and piRNA target genes, which allow functional annotation of the up- and downregulated ncRNA targets [14].

EVs are reported to modulate the neuroimmune system, including maintenance and repair of the BBB, neurogenesis, and synaptic plasticity [15–19]. Due to their role in intercellular communication, EV isolation and characterization have emerged as a method for improving the specificity of biomarker detection. Recent meta-analyses of biomarkers in AD have found that isolating EVs prior to quantifying protein load provides a more specific diagnosis [20].

There is preliminary evidence of *in vivo* FUS-BBBO-induced increases in neuronal EV concentration in blood and *in vitro* FUS-induced increases in neuroprotective EV concentration and glioma-derived EVs [21–23]. Additionally, work outside the CNS has identified a FUS-induced increase in anti-inflammatory EVs after treatment of arthritis [24,25]. Given this preliminary evidence of FUS-BBBO affecting EV concentration and content, as well as their dual role in modulating the neuroimmune system, and as an emerging biomarker, we aimed to study in greater detail the effect of FUS-BBBO on EV concentration and content, and the potential of EV-based liquid biopsy to be translated to the clinic.

While most studies on FUS-enhanced liquid biopsy focus on detecting brain tumor biomarkers in the circulation, there is a plethora of indications where liquid biopsy can be improved with FUS-BBBO. Neurodegenerative diseases, such as AD, are interesting candidates for liquid biopsy, as diagnosis and monitoring of these conditions are often limited to subjective neurological exams, or PET imaging for the detection of molecules such as beta-amyloid and hyperphosphorylated tau, which subject the patients to high doses of ionizing radiation. Identifying biomarkers for AD present in circulation, and developing ways to enhance their concentration could offer a cost-effective and noninvasive way for disease diagnosis and monitoring. Recently, our group conducted a phase I clinical trial (NCT04118764) on six AD patients using our neuronavigation-guided FUS-BBBO system [26], which offered a unique opportunity to study the effect of FUS-BBBO on the concentration of AD-relevant molecules in the blood circulation. We therefore aimed to evaluate the effectiveness of FUS-BBBO in improving liquid biopsy in AD, and assess the clinical applicability of EV-based liquid biopsy in neurodegenerative diseases.

In this study, we explore the response of EVs in serum following FUS-BBBO in a mouse model and in a clinical trial with AD patients. In the mouse study, the concentration of EVs in serum, as well as their transcriptomic and proteomic content, was analyzed. To assess the role of EVs in modulating the neuroimmune response following FUS-BBBO, we investigated the effect of GW4869, a neutral sphingomyelinase inhibitor that blocks EV generation [27], on the restoration timeline of the BBB. Finally, to elucidate the potential of EVs in amplifying neurological marker detection, we collected blood samples from AD patients participating in our group's clinical study on neuronavigation-guided FUS-BBBO and analyzed the protein content of EVs for important AD biomarkers. This study provides the first translational analysis of EV concentration and content after FUS-BBBO, providing evidence of both the EV role within the neuroimmunotherapeutic response and the potential use of isolating EVs to improve FUS-BBBO neurological biomarker accentuation.

Materials and methods

FUS-BBBO in mice

All animal studies were first reviewed and approved by the Institutional Animal Care and Use Committee at Columbia University. Mice in the FUS-BBBO and microbubble (MB) sham groups were anesthetized with a mixture of oxygen and 1%–2% isoflurane (SurgiVet, Smiths Medical PM, Inc., WI), placed on a stereotaxic apparatus (David Kopf Instruments, Tujunga, CA) and their heads were immobilized and depilated to reduce acoustic impedance mismatch. Degassed ultrasound gel was applied to the head and a bath with degassed, deionized water was lowered on top of the head. The lambdoid suture was identified, and the transducer was positioned over it as previously described [28].

In mice that were treated with FUS-BBBO, a single-element, spherical-segment concave FUS transducer (center frequency: 1.5 MHz, focal depth: 60 mm, radius: 30 mm; Imasonic, France) that was driven by a function generator (Agilent Keysight 33220A, Palo Alto, CA, USA) through a 50-dB power amplifier (325LA, Electronic Navigation Industries, Rochester, NY, USA) was used to treat the two hippocampi. The center of the transducer held a pulse-echo ultrasound transducer (V320, center frequency: 7.5 MHz, focal depth: 52 mm, diameter 13 mm; Olympus NDT, Waltham, MA) that was used for alignment and passive monitoring of microbubble cavitation. The pulse-echo ultrasound transducer was driven by a pulser-receiver (5077 PR, Olympus, Waltham, MA, USA) which was in turn connected to a digitizer (Gage Applied Technologies, Inc., Lachine, QC, Canada). The transducer setup was attached to a three-dimensional positioning system (Velmex Inc., Lachine, QC, Canada). Each hippocampus was sonicated first for 10 seconds to obtain a baseline cavitation dose and then again for 2 minutes for the experimental sonication. For all experiments, in-house synthesized, lipid-shelled microbubbles (average concentration: 8 × 10e8/mL, mean diameter: 1.4 μm) were manufactured according to previously published protocols [29,30]. A bolus of 3 μL of microbubbles was diluted in 100 μL of sterile saline and was injected intravenously between the baseline and experimental sonications. The transducer was not triggered to treat the MB sham mice; otherwise, the treatment was identical to that of the FUS-BBBO mice. Mice in the naïve group were not subjected to anesthesia, FUS or microbubble injections.

Mouse serum collection

Mouse blood was collected from the submandibular vein without anesthesia the day before, and 1 hour after FUS-BBBO (Fig. 1a). Mice were held by grasping the skin behind the head firmly. A 16-gauge needle was inserted into the submandibular vein and then removed. Less than 100 μL of blood was collected in heparin-coated serum-separating tubes (Ram Sciences). After collection, gentle pressure was applied to the site of the puncture in order to stop bleeding. The blood was then left at room temperature for 15–30 minutes to clot and then spun down at 3000 x g for 15 minutes. Serum was aliquoted into a separate tube and stored at −80°C for future processing.

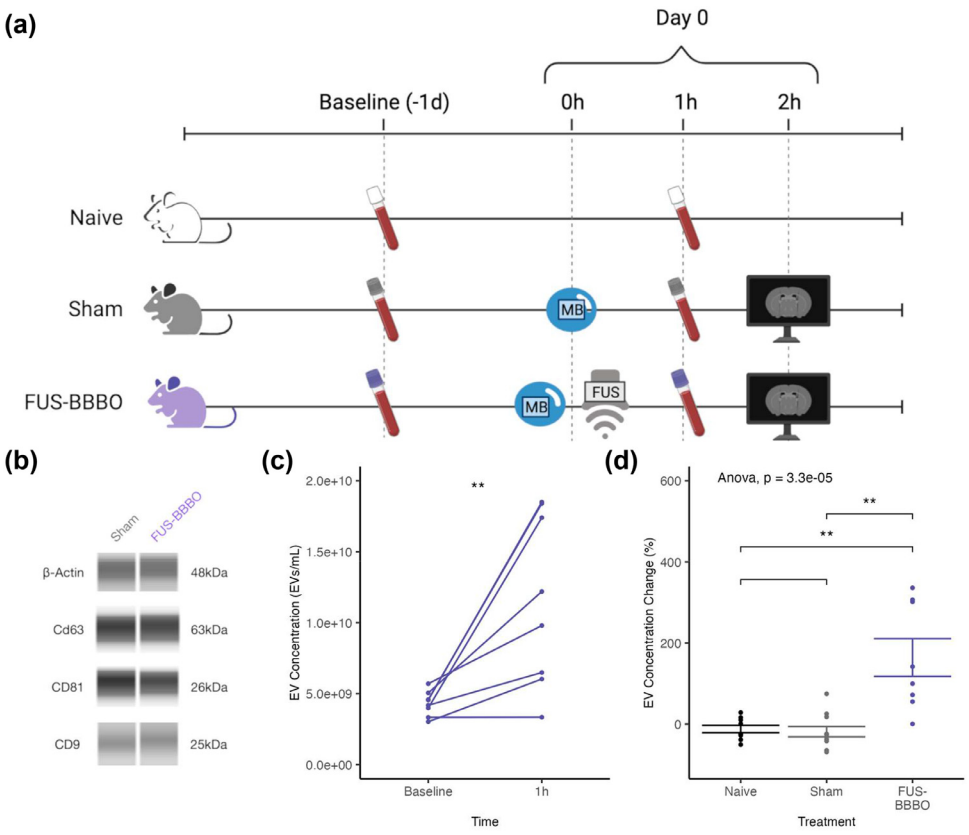

Figure 1. Extracellular vesicle concentration increases after FUS-BBBO in the serum of mice. (a) Murine experimental timeline. Blood draws were taken for EV isolation at two time points: prior to treatment (baseline) and 1 hour after treatment (1 hour). Animals were randomly split into three treatment groups: FUS-BBBO, sham, and naïve. Mice in the FUS-BBBO group had 2 minutes of FUS applied bilaterally following MB injection at time 0. Animals in the sham group were injected with MB, but no FUS was applied. Mice from the FUS-BBBO and sham groups were injected with gadolinium (Gd), and a T1-Weighted MRI was performed less than 2 hours after the FUS-BBBO and sham procedures. Animals in the naïve group were anesthesia-, MB-, and FUS- naïve. (b) Western blots of β-actin and EV tetraspanin markers CD9, CD63, and CD81 on representative sham and FUS-BBBO EVs from 1 hour post-treatment show successful EV isolation. (c) EV concentration at baseline and 1 hour post-treatment in mouse serum. Paired t-test was performed and displayed on a graph. (d) Percent change in EV concentration at the 1-hour time point for all 3 groups; the FUS-BBBO group shows a significant change in EV concentration after 1 hour compared to the naïve and sham groups. One-way ANOVA followed by a Bonferroni-corrected t-test between groups was performed. All statistics are displayed on the graph.

Magnetic resonance imaging for mice

Following treatment and blood draws, all FUS-BBBO and MB Sham animals underwent scanning with a 9.4 T MRI system (Bruker Medical, Boston, MA). Mice were intraperitoneally injected with 0.2 mL of gadodiamide solution (Omniscan^{TM}, GE Healthcare, Princeton, NJ) exactly 30 minutes prior to scanning. Images were acquired using a T1-weighted 2D FLASH sequence (TR/TE 230/3.3 ms, flip angle: 70°, number of excitations: 6, field of view: 25.6 mm × 25.6 mm).

GW4869 drug administration

For the EV inhibition study the drug GW4869 (MedChem Express, Monmouth Junction, NJ, USA), a neutral sphingomyelinase inhibitor, was used to block EV generation. Mice were separated into four groups: naïve, naïve + GW4869, FUS-BBBO, and FUS-BBBO + GW4869. A 2.5 mg/mL stock solution of GW4869 in dimethyl sulfoxide (DMSO) was prepared and stored at −20°C until the day of injection. Immediately before administration, the drug was further diluted in sterile saline to a final concentration of 0.25 mg/mL. Then, the drug was administered intraperitoneally at a dose of 2.5 μg/g body weight per mouse.

To study the effect of EVs in the restoration of the BBB following FUS-BBBO, mice in the FUS-BBBO and FUS-BBBO + GW4869 were monitored for five days after the sonication procedure. The FUS-BBBO + GW4869 group received injections of GW4869 before the FUS-BBBO treatment, and then on day 2 and day 4 after the procedure. The progress of BBBO restoration was monitored for both groups by contrast-enhanced T1-weighted MRI 2 hours after FUS-BBBO, and then on days 1, 3, and 5 post FUS-BBBO. Blood was collected on the day prior to FUS-BBBO, and then 1 hour and 1 day after FUS-BBBO, and always before the injection of gadolinium solution for MRI contrast.

To elucidate the role of EVs in the inflammatory response following FUS-BBBO, mice from all four groups were allowed to survive for one day after the FUS-BBBO groups were sonicated. Mice in the naïve + GW4869 and FUS-BBBO + GW4869 groups received one injection of the drug immediately before the FUS-BBBO procedure took place. Furthermore, BBBO was confirmed in the mice that underwent FUS-BBBO by contrast-enhanced MRI 2 hours after the sonication procedure. Mice from all groups had blood taken on the day prior to FUS-BBBO, 1 hour, and 1 day after FUS-BBBO. After the final blood draw, the mice were sacrificed by transcardial perfusion with cold 1X PBS and their hippocampi were separated for bulk RNA sequencing.

FUS treatment in AD patients

Six Alzheimer's Disease (AD) patients underwent neuronavigation-guided FUS-BBBO as part of our phase I clinical trial (NCT04118764). All methods used were first approved by Columbia University's Institutional Review Board and all participants provided informed consent prior to the FUS-BBBO procedure. Inclusion criteria, apart from

diagnosis of AD, included a positive ^{18}F-Florbetapir PET imaging, as well as a Mini-Mental State Exam (MMSE) score between 12 and 26, which aimed to include subjects with mild to moderate cognitive impairment [31]. A complete list of the inclusion and exclusion criteria is given in our group's recent publication from this clinical trial [26]. The right frontal lobe was targeted and numerical simulations using the k-wave package in MATLAB were carried out prior to the experiment to estimate the power attenuation of FUS through the skull. A detailed account of the methods of FUS-BBBO in AD patients is given in our group's clinical paper [26]. Briefly, a single-element, spherical-segment FUS transducer (H-231, Sonic Concepts, Bothell, WA, USA) was driven at a frequency of 0.25 MHz by a function generator (Agilent, Palo Alto, CA, USA) and a 50-dB power amplifier (Electronic Navigation Industries, Rochester, NY, USA) to emit FUS pulses with pulse length 10 ms and pulse repetition frequency 2 Hz. A derated peak-negative FUS pressure of 200 kPa (mechanical index (MI) = 0.4) was applied for 2 minutes. A bolus of microbubbles (0.1 mL/kg, Definity, Lantheus) was intravenously injected at the start of the sonication. During the sonication, the cavitation dose was monitored by using a single-element transducer for the first four patients and an imaging array transducer (P4-2, ATL Philips) for the remaining two patients.

Patient BBBO volume quantification

BBB opening volume was quantified from the contrast-enhanced T1-weighted MRIs, which were taken 2 and 72 hours after FUS-BBBO using a 3T system (Signa Premiere, General Electric, Boston, MA, USA) for the confirmation of the opening and closing of the BBB, respectively. For T1-weighted contrast enhancement, an intravenous injection of 0.2 mL/kg gadoterate meglumine (Dotarem®, Guerbet). The contrast-enhanced volume was quantified by subtracting the 72-hour contrast-enhanced T1 MRI from the 2-hour MRI and thresholding the subtracted image. The threshold was chosen automatically so that the average intensity within the opening volume was considerably higher than that of the surrounding area, with a 98% level of confidence assuming the Gaussian distribution of the intensity of the subtracted image.

Extracellular vesicle isolation

The commercial ExoQuick (Systems Biosciences, Palo Alto, CA, USA) was used according to manufacturer instructions to isolate extracellular vesicles from both mouse and human serum. The ExoQuick precipitation method was chosen over ultracentrifugation to simplify the isolation process, despite the latter being the gold standard for high extracellular vesicle yield and purity [32]. Briefly, 25 μL of mouse serum was diluted with 75 μL of 1X PBS before incubation with 22.5 μL of ExoQuick for 30 minutes at room temperature. For human samples, 200 μL of undiluted serum was incubated with 45 μL of ExoQuick for 30 minutes at room temperature. The samples were then spun down at 1500 × g for 35 minutes at 4°C, and the pellet (isolated extracellular vesicles) was resuspended in 100 μL or 200 μL of 1X PBS for the mouse and human samples respectively. The isolated EV suspensions were stored at −80°C until further processing.

Nanoparticle tracking analysis

Extracellular vesicle concentration analysis was quantified by nanoparticle tracking analysis (NTA) on a NanoSight (NS300, Malvern Panalytical, Malvern, UK). 5 μL of isolated mouse EVs or 1 μL of isolated human EVs were further diluted into 1 mL of 1X PBS. This solution was then run through the Nanosight at a rate of 1000 μL/min, and the resulting image was captured and analyzed for particle concentration and size distribution. The relative concentration changes between baseline and post-FUS-BBBO time points for each subject were subsequently assessed.

Multiplex protein quantification

For the samples from the clinical study, a Luminex multiplex assay was used to quantify proteins in serum and isolated clinical extracellular vesicles (Luminex Corporation, Austin, TX, USA). A simpler and more cost-effective assay was used for the clinical study as opposed to mass spectrometry to allow for an easier transition to the clinic. Single procartaplex kits were purchased and combined to make a custom multiplex panel for analysis (Invitrogen, Waltham, MA, USA). Data were fit with a separate five-parameter logistic dose-response curve for each protein, and all curves had R^2 greater than or equal to 0.95.

Mass spectrometry protein analysis

For the samples from the mouse studies, mass spectrometry proteomics was performed by Systems Biosciences on already isolated EVs. In brief, Systems Biosciences lysed the isolated EVs in a gel-loading buffer, followed by gel-based extraction and trypsinization for peptide library creation for LC/MS ESI-TOF. Peptide signatures were then mapped to a database of known protein sequences. Peptide quantification across all four runs was loaded into R, normalized, and processed for differential protein expression utilizing the UniprotR package. All functional annotation was performed with the TopGO package.

RNA sequencing

RNA Sequencing was performed by Systems Biosciences on already isolated EVs and dissected frozen hippocampus tissue. RNA was isolated and quantified using Agilent Bioanalyzer Small RNA Assay before 75 bp single-end read Next Gen Sequencing libraries were prepared using Qiagen small RNA library preparation and gel purification. Sequencing was performed on Illumina NextSeq with SE75 at an approximate depth of 10−15 million reads per sample. Reads were processed and aligned to the GRCm38 genome with Ensemble transcriptome annotation (GRCm38.p6) using CellRanger with default parameters. Count tables were loaded into R and underwent normalization and differential gene expression analysis using the edgeR package. piRNA and miRNA targets were extracted from piRNAdb and miRBase, respectively. All functional annotation was performed with the TopGO package.

Western blotting

RayBiotech performed western blotting using an automated capillary immunoassay method. Samples and reagents were loaded onto an assay plate and put into a western blotting machine. The sample was automatically loaded and separated by size while it traveled through the stacking and separation matrix. Then, the separated proteins are fixed with proprietary capture chemistry. Target proteins are identified with primary and secondary HRP-conjugated antibodies. Details on the Western Blot service, and the antibodies used can be found on the website of RayBiotech (www.raybiotech.com/other-services/western-blot-service or by searching "Auto-Western Blot Service RayBiotech").

Statistical analysis

Statistical analysis was carried out using GraphPad Prism (GraphPad Software Inc, La Jolla, CA, USA). The differences in EV concentration before and after FUS-BBBO in mice and AD patients were assessed by paired t-tests, and linear regression analysis was carried out to correlate the BBB opening volume with the 3-day EV concentration change and the log-fold change in biomarker content in serum and EVs of AD patients. The difference in content between serum and isolated EVs was assessed using an unpaired t-test. In the GW4869 EV depletion study, the differences between groups were

assessed by one-way ANOVA followed by Bonferroni post hoc multiple comparison correction. For RNA-sequencing, statistical analysis was carried out on R using a quasi-likelihood F test (QLF) using the glmQLFTest function and a coefficient of 3. Statistical significance was set for $p<0.05$.

Results

Murine extracellular vesicle concentration increases after FUS-BBBO

Wild-type mice were separated into three groups – naïve, sham, and FUS-BBBO (Fig. 1a). Animals treated with FUS-BBBO were intravenously injected with microbubbles (MB) and treated with 2 minutes of focused ultrasound bilaterally on the hippocampi, consistent with literature [28,33]. Animals in the sham group were intravenously injected with MB but were not treated with focused ultrasound. Animals in all groups had blood drawn twice immediately before treatment (baseline) and 1 hour after treatment (1 hour). Animals in the sham and FUS-BBBO groups underwent contrast-enhanced T1-weighted MRI after the second blood draw to confirm the opening within the FUS-BBBO group and the lack of opening within the sham group. The methods detail EV isolation and concentration quantification.

Western blots of the isolated EVs from representative sham and FUS-BBBO samples confirmed the successful isolation of the EVs via expression of the marker tetraspanin proteins CD9, CD81, and CD63, and using β-actin as a control (Fig. 1b). Nanoparticle tracking analysis (NTA) reveals that the EV concentration is significantly increased 1 hour after treatment compared to the baseline (Fig. 1c). Furthermore, the average increase of 164% after FUS-BBBO is significantly higher than the percentage change in naïve and sham samples which averages near 0% (Fig. 1d), with 95% confidence intervals between 81.75% and 271.3% for naïve vs FUS-BBBO, and 92.38% and 273.6% for sham vs FUS-BBBO.

FUS-BBBO alters murine extracellular vesicle protein and RNA load

Given the significant increase in EV concentration 1 hour after treatment, we performed whole genome RNA-sequencing and mass spectrometry protein identification (Systems Biosciences, Palo Alto, CA, USA) on isolated EVs from baseline and 1 hour. To reduce the effects of inter-subject variability, isolated EV samples from 3 animals from each time point (baseline and 1-hour post-FUS-BBBO) were pooled and underwent both processes. Differential gene expression analysis between 1 hour and baseline reveals significantly up- and downregulated protein-coding and non protein-coding (ncRNA) RNAs (Fig. 2a–c).

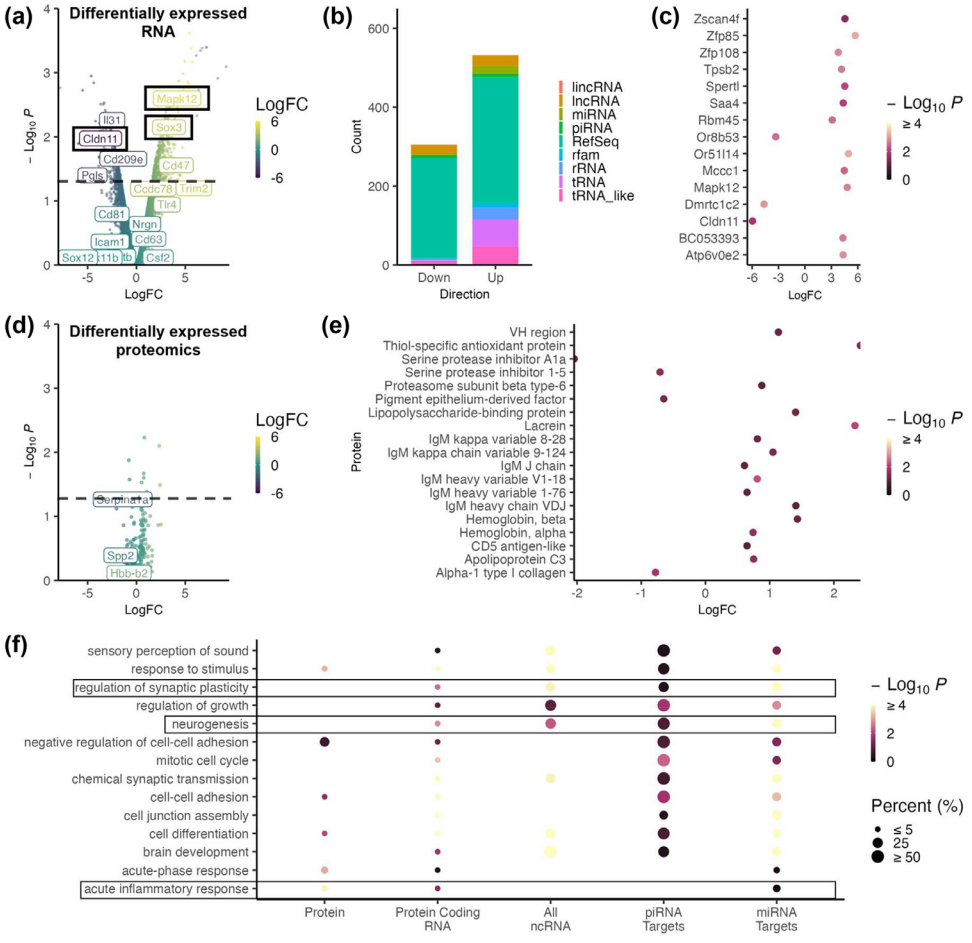

Figure 2. FUS-BBBO alters the murine EV RNA and protein load. (a) Volcano plot of differentially expressed RNA between 1 hour post-treatment and baseline EVs with key protein-coding genes highlighted. Genes above the dashed line are significantly ($p<0.05$) differentially expressed. (b) A bar chart of the significantly ($p<0.05$) up and down-regulated RNA split by type. c) Plot of the most significantly up and downregulated protein-coding RNAs with LogFC of protein expression on the horizontal axis. (d) Volcano plot of differentially expressed proteins (from mass spectrometry proteomics) between 1 hour post-treatment and baseline EVs with key proteins highlighted. Proteins above the dashed line are significantly ($p<0.05$) differentially expressed. (e) Plot of the most significantly up- and downregulated proteins with LogFC of protein expression on the horizontal axis. (f) Functional annotation of the 1) significantly upregulated protein, 2) significantly upregulated protein-coding genes, 3) significantly upregulated noncoding RNA (ncRNA), 4) genetic targets of the significantly upregulated piRNA, and 5) genetic targets of the significantly upregulated micro-RNA (miRNA). The adjusted Kolmogorov-Smirnov p-value magnitude is displayed in color. The size of each dot corresponds to the percentage of annotated genes from that term that are significantly upregulated.

Upregulated protein-coding genes detected via RNA sequencing include proliferation-associated genes such as *Sox3* and inflammation-associated genes such as *Mapk12*. Downregulated protein-coding genes include tight-junction genes such as *Cldn11*. Additionally, noncoding RNA types such as microRNA (miRNA) and transfer RNA (tRNA) are also upregulated (Fig. 2b). These types of noncoding RNA are known for regulating gene expression and protein synthesis. Differential expression of the protein identification finds many fewer significantly up and downregulated proteins (only 10 proteins compared to 900 genes). The most significantly upregulated proteins include immediate inflammatory response proteins such as *Lbp* and hemoglobin-associated proteins such as *Hbb-bs* (Fig. 2d–e).

Next, functional annotation was used to identify the biological processes associated with the differentially expressed: a) proteins, b) protein-encoding genes, c) ncRNA, d) piRNA target genes, and e) miRNA target genes. Protein functional annotation maps to immediate and acute inflammatory responses, while protein-coding and noncoding RNA correspond to more long-term responses such as synapse regulation and neurogenesis (Fig. 2f). Many of the functions associated with the RNA changes are coincident with reported FUS-BBBO increases in neurogenesis [5], proliferation [5], and synaptic remodeling [13]. This leads to the hypothesis of the EV response involvement in the neuroimmunotherapeutic responses to FUS-BBBO.

GW4869 eliminates murine EV concentration increase and reduces inflammatory response

To further elucidate the role of EVs in modulating FUS-BBBO neuroimmunotherapy, we utilized GW4869, a neutral sphingomyelinase inhibitor that is the most widely used agent for blocking EV generation [27] (Fig. 3a). We studied four groups for this experiment: naïve, naïve + GW4869, FUS-BBBO, and FUS-BBBO + GW4869.

First, we confirmed that GW4869 successfully eliminated the FUS-BBBO-induced increase in EV concentration. We found that 1 hour after treatment, the animals treated with FUS-BBBO + GW4869 had a statistically lower EV concentration compared to baseline, starkly contrasting with our FUS-BBBO group, which increased in EV concentration by over 100% (Fig. 3b). Comparing the EV concentration change between our four groups, we see that FUS-BBBO + GW4869 is indistinct from naïve and naïve + GW4869 both 1 hour and 1 day after treatment (Fig. 3c).

Next, we monitored BBB restoration after FUS-BBBO with and without GW4869. The BBB opening volume of each animal was quantified on Days 0, 1, 3, and 5. On every day of measurement, the animals in the FUS-BBBO + GW4869 had smaller openings than those in the control group (Fig. 3d). This difference is particularly significant on day 1 when the BBBO volumes of the FUS-BBBO and FUS-BBBO + GW4869 groups averaged 58% and 42% of the day 0 BBBO volume respectively (Fig. 3e).

Due to previous literature identifying 1 day as the peak of FUS-BBBO-induced inflammation [5,34,35], and given the more restored BBB in our FUS-BBBO + GW4869 group at this time point, we performed bulk RNA sequencing on hippocampus tissue extracted from 1 day after FUS-BBBO for our four treatment groups. Differential gene expression between FUS-BBBO and FUS-BBBO + GW4869 revealed that GW4869 reduced the presence of inflammatory markers, including *IL6* and *CCL4* (Fig. 3f). In order to account for any effects of GW4869 treatment alone, we performed functional annotation on the differentially expressed genes between FUS-BBBO compared with naïve and FUS-BBBO + GW4869 compared with naïve + GW4869. This revealed increased processes altered in FUS-BBBO without injecting GW4869, including migratory, development, and inflammatory terms. The functions shared by both comparisons are primarily involved with vasculature development (Fig. 3g).

Overall, we see that GW4869 eliminates the FUS-BBBO-induced increase in EV concentration, decreases the volume of BBB opening, and reduces the number of differentially affected processes after FUS-BBBO, indicating a vital role for EVs within the neuroimmunotherapeutic response to FUS-BBBO.

Patient extracellular vesicle concentration peaks 1 hour after FUS-BBBO

Six Alzheimer's Disease Patients underwent FUS-BBBO as part of our group's phase I clinical trial (NCT04118764) as reported in our group's clinical paper [26]. All patients had blood drawn immediately prior to treatment (Baseline) and 3 days after treatment. Additionally, the last four patients — P3, P4, P5, and P6 — had blood drawn 1 hour after treatment (Fig. 4a). All patients apart from P3 had confirmed blood-brain barrier opening; due to failed microbubble injection, P3 did not have successful opening, as determined by the absence of contrast enhancement in T1-weighted MRI imaging and thus is considered a FUS-sham subject. Furthermore, the procedure was well tolerated by all patients, and no patients showed any severe adverse events, while only one patient (P1) exhibited a mild skin erythema presented on day 0 (treatment day) and an asymptomatic cerebral edema with a superficial hemorrhagic component which presented on day 3. Follow-up of this patient 15 days post-FUS-BBBO revealed that the radiological signs of the edema had been fully resolved. Full details of the clinical findings of this study have been published by Bae et al. [26].

EVs were isolated from each time point for each patient. Western blotting of the isolated EVs from representative Baseline and FUS-BBBO samples confirmed successful EV isolation (Fig. 4b). Comparing EV concentration from Baseline to 1 hour post-treatment reveals a significant increase in EV concentration (Fig. 4c) with a near-return to Baseline by 3 days after treatment (Fig. 4d). Furthermore, the percent increase in EVs 3 days after treatment is correlated with the volume of the blood-brain barrier opening (Fig. 4e).

EV isolation improves FUS-BBBO amplification of neurological biomarkers

To elucidate the utility of EVs in improving liquid biopsy specificity, we quantified several potential AD biomarkers, EV proteins, and other CNS proteins within our patient-isolated EVs, isolated EVs normalized by EV concentration (normalized EVs), and total serum. The concentration of the target biomarkers and proteins in the total EV population, normalized EV population as well as total serum was found to remain mostly unchanged 1 hour after treatment and even decreased compared to baseline. Three days after treatment, the concentration of a number of proteins is significantly increased for both EVs and normalized EVs compared to the total serum, which has no changes in marker concentration for any of the markers (Fig. 5a). Furthermore, the differences between 1 hour and 3 days log fold change (LogFC) in protein content are more statistically distinct for the EVs and normalized EVs than for total serum (Fig. 5b).

Finally, in our clinical study, we compared the MRI-based blood-brain barrier opening volume to the LogFC of select biomarkers 3 days after treatment [26]. Thorough analysis of this data indicated that the level of AD biomarkers is positively correlated with BBBO in serum and EV content but not normalized EV content (Fig. 5b). This indicates that the increase in biomarker detection is due to a higher number of EVs being released as opposed to each EV having a higher biomarker concentration. Overall, our findings from the AD clinical trial reveal the potential of FUS-BBBO in enhancing EV-based biomarker detection sensitivity and specificity for liquid biopsy in AD.

Discussion and conclusion

Focused ultrasound blood-brain barrier opening (FUS-BBBO) has been studied as a neuroimmunotherapeutic and a method of improving liquid biopsy specificity for neurological disorders [4,6,11]. Due to the dual role of EVs in modulating the neuroimmune system [18,19] and as an emerging biomarker [20,36], we aimed to identify the effect of FUS-BBBO on EVs isolated from mouse and AD patient serum.

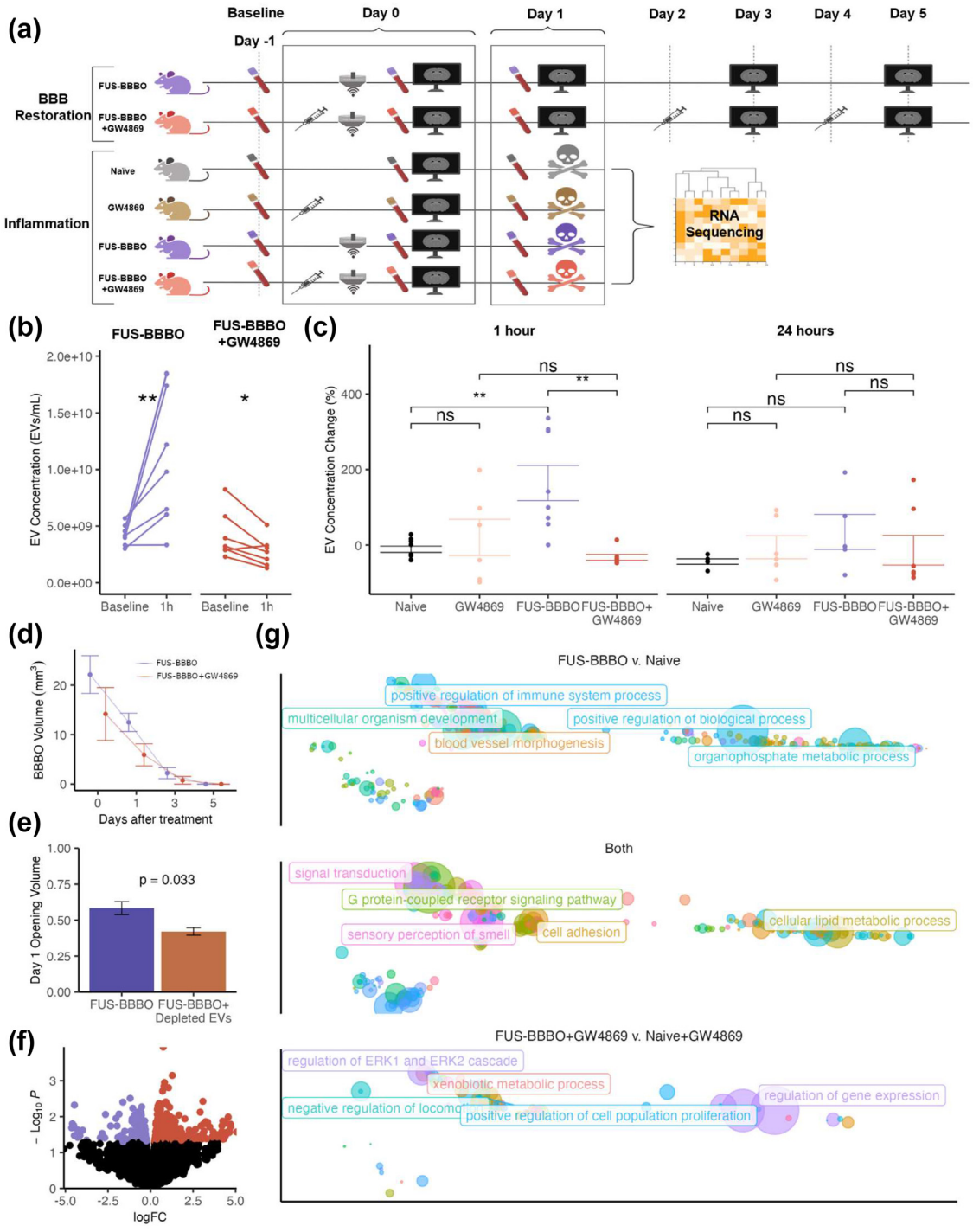

Figure 3. GW4869 eliminates murine EV concentration increase and reduces inflammatory response. (a) GW4869 study timeline. In the BBB restoration study, sequential MRIs were taken after FUS-BBBO to monitor BBB restoration after treatment with and without GW4869. In the inflammation study, animals were sacrificed 1 day after treatment and the inflammatory response and bulk transcriptome were compared between FUS-BBBO, FUS-BBBO + GW4869, naïve and naïve + GW4869 animals. (b) EV concentration at Baseline and 1 hour after treatment with either FUS-BBBO or FUS-BBBO + GW4869. Paired t-test was performed for each group. (c) Percent change in EV concentration 1 hour and 1 day after treatment for all groups. ANOVA followed by Bonferroni post hoc t-tests were performed for each time point. (d) BBBO volume for the day of treatment and 1 day, 3 days, and 5 days following treatment for both FUS-BBBO and FUS-BBBO + GW4869. (e) The proportion of the original BBBO volume that is still open 1 day after treatment for animals in the restoration study. An unpaired t-test was performed between the two groups. (f) Volcano plot comparing the profile of FUS-BBBO + GW4869 and FUS-BBBO hippocampi. Significantly expressed ($p<0.05$) genes are colored. (g) Significantly upregulated terms from differential gene expression analysis between FUS-BBBO + GW4869 and naïve + GW4869 and FUS-BBBO compared with naïve. Functional ontology terms are clustered by similarity, and the point size shows their significance. Terms appearing in both functional annotations are shown in the "Both" panel with the average significance between the two comparisons.

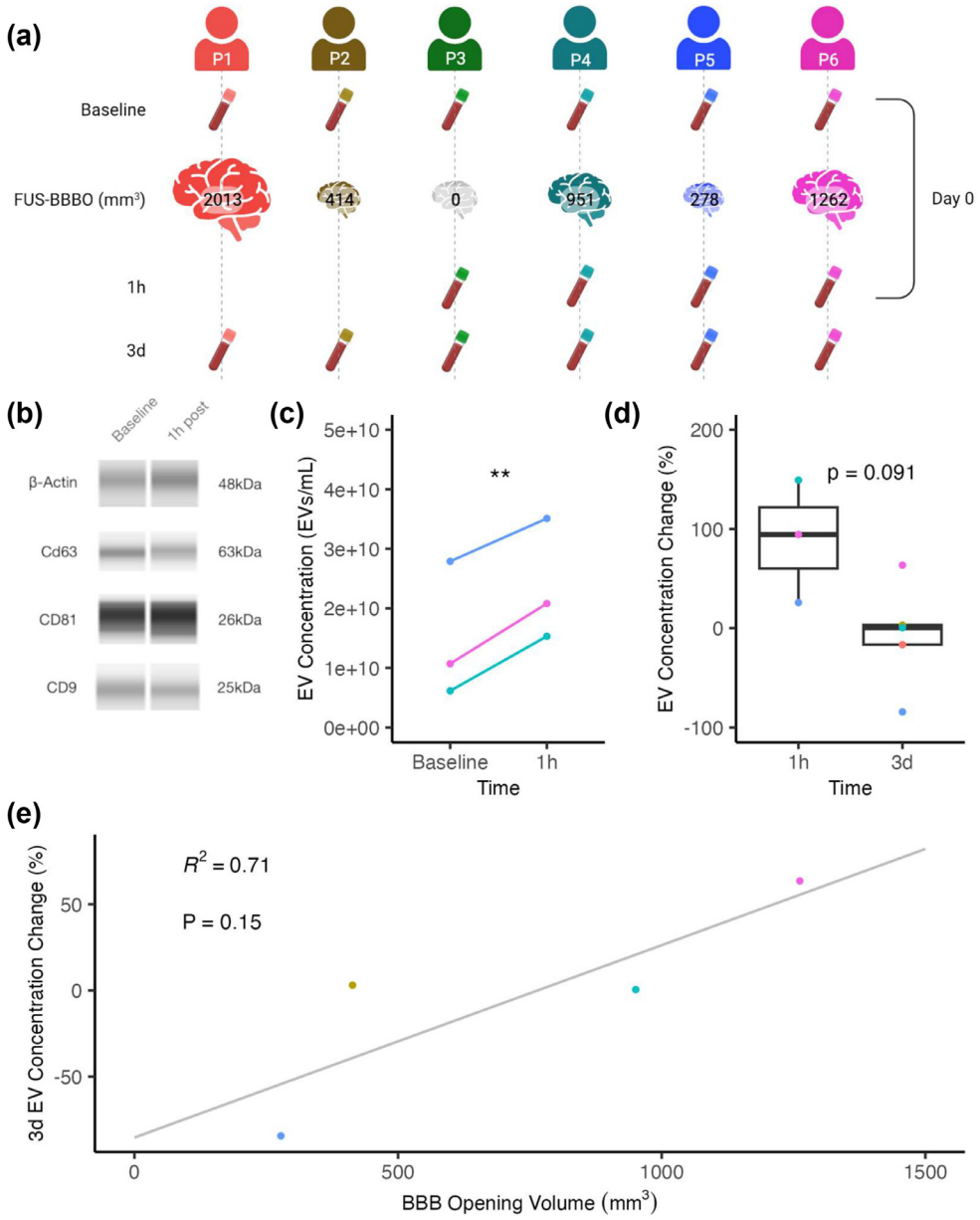

Figure 4. Extracellular vesicle concentration increases after FUS-BBBO in Alzheimer's Patients. (a) Schematic of the clinical trial with neuronavigation-guided FUS-BBBO, including each patient's blood draw and opening volume. (b) Western blots of β-actin and tetraspanins CD63, CD81, and CD9 from isolated EVs at baseline and 1 hour after FUS-BBBO confirm successful EV isolation. (c) EV concentration at Baseline and 1 hour after treatment for the patients who had successful treatment sessions. The differences between the two time points are statistically significant, following a paired t-test ($p<0.01$) (d) Percent change in EV concentration 1 hour and 3 days after treatment compared to baseline. An unpaired two-tail t-test was performed between the two groups, and the differences were found to be not statistically significant, but trending towards significance ($p=0.091$). (e) Correlation of BBBO volume and the percent change in EV concentration 3 days after treatment. Simple linear regression was performed, and the resulting R^2 and p-value are on the chart. While the p-value indicates lack of statistical significance ($p>0.05$), these results show a good correlation between the BBBO volume and EV concentration change 3-days post-BBBO.

We first identified a significant increase in mouse EV concentration 1 hour after treatment coincident with RNA changes associated with the EV-dependent neuroimmunotherapeutic effects of FUS-BBBO such as neurogenesis, synaptic pruning, and barrier maintenance [5,6,16,37,38]. Restricting the EV concentration increase with GW4869 resulted in reduced blood-brain barrier opening volume and inflammation, indicating the contribution of the EVs to FUS-BBBO inflammation and opening volume. This result also points to an active role that EVs may have in the immunotherapeutic response of FUS-BBBO, as EVs are contributing to the intercellular exchange of inflammatory signals. Future studies will aim to map the transcriptomic and proteomic changes exhibited by EVs following FUS-BBBO to specific neuroinflammatory and neuroprotective pathways to further understand the cellular responses to FUS-BBBO.

The immune response to FUS-BBBO has spearheaded debate about the method's safety, so the ability to control and mitigate FUS-BBBO-induced inflammation provides an exciting new avenue, mainly when FUS-BBBO is used purely as a drug delivery tool [35]. In particular, EV modulation and depletion could be used to reduce or fine-tune the inflammatory response to FUS-BBBO in drug and gene delivery applications where an immune response may be undesirable, or even to controllably amplify the inflammatory response

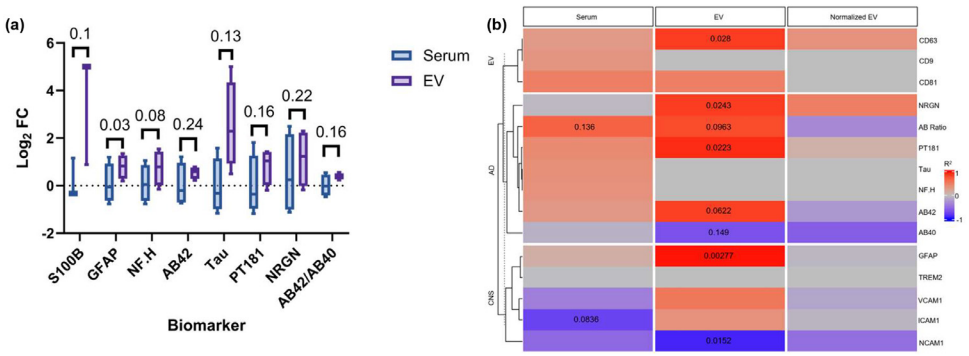

Figure 5. EV isolation further improves FUS-BBBO amplification of neurological biomarkers. (a) Comparison of the FUS-BBBO-induced increase in neurological biomarker detection in total serum (blue) and isolated EVs (purple) with a paired t-test performed for each biomarker. (b) Correlation between FUS-induced volume of opening and the LogFC change of biomarkers in total serum, isolated EVs and isolated EVs normalized to the EV concentration (Normalized EV). Simple linear regression was performed for each condition, and the R2 and p values are displayed on the heatmap.

in drug-free applications such as FUS-BBBO immunotherapy. Future work will include investigating the neuroimmunotherapeutic capacity of FUS-BBBO with depleted EVs because those benefits may require a complete neuroimmune response.

Secondly, we identified a significant increase in Alzheimer's Disease (AD) patient EV concentration 1 hour after treatment that increased linearly with the BBBO volume 3 days after treatment. This was accompanied by increased AD biomarker detection specificity in isolated EVs compared to total serum, which was also correlated with the volume of BBBO as shown in our clinical study [26]. Combined, these results highlight the potential of EVs to be used as accurate and specific markers for neurological diseases, and the ability of FUS-BBBO to amplify their detection in a noninvasive way. These results complement prior studies exploring the role of EVs in neurodegenerative diseases, as amyloid and tau transport in EVs has been previously observed, and plasma exosomes have been previously proposed as biomarkers for AD as well as other neurodegenerative diseases such as Parkinson's and Huntington's Disease [39].

The results of this study may inform future clinical applications of EV-based liquid biopsy for neurodegenerative diseases. While complete replacement of costly monitoring methods, such as PET and MRI imaging, by liquid biopsy is not yet feasible, the use of EVs can complement imaging and potentially provide additional information on the presence of disease-related molecules in the brain. In particular, since liquid biopsy can be multiplexed for the detection of multiple proteins from a single sample, it may provide a more complete view of the molecular state of the disease, without needing multiple imaging sessions and increased radiation exposure, as is the case with PET imaging. EVs may also be used as diagnostics in cases where approved PET contrast agents are not yet available, paving the way for applications in a plethora of neurodegenerative diseases. However, clinical adoption of FUS-BBBO-enhanced liquid biopsy still requires multiple steps to be completed, such as regulatory approval of FUS-BBBO for different neurological conditions, development of reliable neurological condition biomarkers, and further refinement of the EV isolation and biomarker detection methods.

One potential limitation of our study relates to the use of ExoQuick as the method for EV isolation. While it is a widely accepted commercial product for facile and scalable isolation of exosomes and microvesicles between 30 and 200 nm, it may also isolate other non-EV components thus reducing the purity of the resulting EV suspension [40]. Additionally, despite following the manufacturer's instructions, differences in batches between ExoQuick formulations, as well as during each isolation process, may add to the variability of results. To further improve results, future studies will involve EV isolation using different methods, such as size exclusion chromatography, which can improve purity and reproducibility without being as time-consuming as ultracentrifugation [41].

An additional limitation related to the use of EVs for liquid biopsy is the inherent variability in EV concentration between subjects. As observed in our mouse studies, the absolute concentrations of EVs were significantly variable between subjects, thus making it difficult to draw conclusions from the absolute values of the EV concentrations. This was also the case in the clinical study, where EV concentration, as well as biomarker content in EVs was variable between subjects. The variability in biomarker concentrations in patients could be indicative of differences in the response of EVs for each individual, making the case for the development of a liquid biopsy model where each subject serves as his or her own control, and biomarker concentrations are measured relatively to the individual's baseline. Using a baseline sample for each subject is therefore of utmost importance, as it allows contextualizing any changes in EV concentration and content and normalizing for inter-subject variability.

While EV content was analyzed for both mice and human subjects, the two studies may not be directly comparable due to the different methods of analyzing protein content in the EVs. While mass spectrometry proteomic analysis gives a detailed account of the proteomic changes in the EVs following FUS-BBBO, a Luminex assay was opted for in the clinical study, due to its potential to be used as a lower cost and clinically translatable method. As such, the information obtained from the two studies regarding the changes in protein content cannot be compared head-on in the present study. Additionally, there may be differences in EV content between the mouse and human studies due to the different disease status of the two species, with a healthy mouse model but an AD human population. In future studies, a comparison between a diseased animal model and the target human population using the same analytical technique could help draw more comparable conclusions between the species.

In order for this technology to be implemented for improving biomarker specificity, there needs to be a method of differentiating between the changes in biomarker concentration due to the treatment itself and those due to the disease. Other groups have addressed this challenge by utilizing disease-specific biomarkers such as circulating tumor DNA (ctDNA), which can indicate the presence of a disease with high specificity [7,9]. This becomes much more complex with diseases such as AD, where many of the proposed biomarkers are CNS proteins that are always in the CNS albeit in different concentrations, and thus can vary significantly between patients [20,36]. Future research on discovery of disease-specific biomarkers for neurodegenerative diseases is essential, and particularly biomarkers that can be indicative of the disease stage, as they may be able to predict clinical outcomes irrespective of FUS-BBBO-induced concentration changes. Additionally, future studies should include a normalization between BBBO and biomarker concentration that can be used to identify a BBBO-induced concentration change compared to a disease-induced concentration change. In this fashion, it will be possible to

untangle the effects of FUS-BBBO from the effects that disease progression may have on biomarker concentration.

Overall, this study presents the first preclinical and clinical evidence of FUS-BBBO increasing EV concentration and altering EV content, which has implications for both the mechanism of FUS-BBBO neuroimmunotherapy and the optimization of FUS-BBBO-induced amplification of neurological disease biomarkers.

Author Contributions

ARKS, AJB, and EEK designed the study and the methodology. ARKS, AJB, and MRD conducted in *vivo* mouse studies. KL and SB collected and processed blood samples from the clinical study. ARKS, FNT, and MRD processed the EV results and made figures. ARKS, FNT, and EEK drafted and revised the manuscript. EEK acquired funding and provided resources for the study. All authors contributed to discussions and reviews of the manuscript.

Conflict of interest

Some of the work in this study is supported by patents optioned to Delsona Therapeutics, Inc. where EEK serves as a co-founder and scientific adviser. The remaining authors declare no competing interests.

Data availability statement

The data that support the findings of this study are available from the corresponding author upon reasonable request.

Acknowledgments

This study was supported in part by the National Institutes of Health under Grants R01AG038961, R01EB009041, and R56AG038961, and the Focused Ultrasound Foundation. FNT was also supported by the Onassis Foundation under contract number F ZT 072-1/2023-2024. Some figures were created with BioRender.com. The authors wish to thank UEIL members Rebecca Noel, Ph.D., Daniella Jimenez, M.S., Samantha Gorman, B.S., and Nancy Kwon M.S. for their support and insightful scientific discussions.

References

[1] Abbott NJ, Patabendige AAK, Dolman DEM, Yusof SR, Begley DJ. Structure and function of the blood-brain barrier. Neurobiol Dis 2010;37:13–25.
[2] Konofagou EE, Tung YS, Choi J, Deffieux T, Baseri B, Vlachos F. Ultrasound-induced blood-brain barrier opening. Curr Pharm Biotechnol 2012;13(7):1332–45.
[3] Stockwell J, Abdi N, Lu X, Maheshwari O, Taghibiglou C. Novel central nervous system drug delivery systems. Chem Biol Drug Des 2014;83(5):507–20.
[4] Zhu L, Cheng G, Ye D, Nazeri A, Yue Y, Liu W, et al. Focused ultrasound-enabled brain tumor liquid biopsy. Sci Rep 2018;8(1):1–9.
[5] Kline-Schoder AR, Chintamen S, Willner MJ, DiBenedetto MR, Noel RL, Batts AJ, et al. Characterization of the responses of brain macrophages to focused ultrasound-mediated blood−brain barrier opening. Nat Biomed Eng 2023;8:650–63.
[6] Karakatsani ME, Kugelman T, Ji R, Murillo M, Wang S, Niimi Y, et al. Unilateral focused ultrasound-induced blood-brain barrier opening reduces phosphorylated Tau from the rTg4510 mouse model. Theranostics 2019;9(18):5396–411.
[7] Pacia CP, Yuan J, Yue Y, Xu L, Nazeri A, Desai R, et al. Sonobiopsy for minimally invasive, spatiotemporally-controlled, and sensitive detection of glioblastoma-derived circulating tumor DNA. Theranostics 2022;27(1):362–78.
[8] Pacia CP, Zhu L, Yang Y, Yue Y, Nazeri A, Michael Gach H, et al. Feasibility and safety of focused ultrasound-enabled liquid biopsy in the brain of a porcine model. Sci Rep 2020;10(1):1–9.
[9] Zhu L, Nazeri A, Pacia CP, Yue Y, Chen H. Focused ultrasound for safe and effective release of brain tumor biomarkers into the peripheral circulation. PLoS One 2020;15(6):1–15.
[10] Rincon-Torroella J, Khela H, Bettegowda A, Bettegowda C. Biomarkers and focused ultrasound: the future of liquid biopsy for brain tumor patients. Journal of Neuro-Oncology, 156. Springer; 2022. p. 33–48.
[11] Mooney SJ, Nobrega JN, Levitt AJ, Hynynen K. Antidepressant effects of focused ultrasound induced blood-brain-barrier opening. Behav Brain Res 2018;342:57–61.
[12] Mooney SJ, Shah K, Yeung S, Burgess A, Aubert I, Hynynen K. Focused ultrasound-induced neurogenesis requires an increase in blood-brain barrier permeability. PLoS One 2016;11(7):1–11.
[13] Noel RL, Gorman SL, Batts AJ, Konofagou EE. Getting ahead of Alzheimer's disease: early intervention with focused ultrasound. Front Neurosci 2023;17:1–16.
[14] Zhang P, Wu W, Chen Q, Chen M. Non-coding RNAs and their integrated networks. J Integr Bioinform 2019;16(3):1–12. doi: 10.1515/jib-2019-0027.
[15] Meldolesi J. Extracellular vesicles (exosomes and ectosomes) play key roles in the pathology of brain diseases. Molecular Biomedicine 2021;2(18):1–13. doi: 10.1186/s43556-021-00040-5.
[16] Zagrean AM, Hermann DM, Opris I, Zagrean L, Popa-Wagner A. Multicellular crosstalk between exosomes and the neurovascular unit after cerebral ischemia: Therapeutic implications. Front Neurosci 2018;12:1–9. doi: 10.3389/fnins.2018.00811.
[17] Zhang L, Graf I, Kuang Y, Zheng X, Haupt M, Majid A, et al. Neural progenitor cell-derived extracellular vesicles enhance blood-brain barrier integrity by NF-κB (nuclear factor-κB)-dependent regulation of ABCB1 (ATP-binding cassette transporter B1) in stroke mice. Arter Thromb Vasc Biol 2021;41(3):1127–45.
[18] Simeone P, Bologna G, Lanuti P, Pierdomenico L, Guagnano MT, Pieragostino D, et al. Extracellular vesicles as signaling mediators and disease biomarkers across biological barriers. Int J Mol Sci 2020;21(7):1–27. doi: 10.3390/ijms21072514.
[19] Marostica G, Gelibter S, Gironi M, Nigro A, Furlan R. Extracellular vesicles in neuroinflammation. Front Cell Dev Biol 2021;8:1–13. doi: 10.3389/fcell.2020.623039.
[20] Soares Martins T, Trindade D, Vaz M, Campelo I, Almeida M, Trigo G, et al. Diagnostic and therapeutic potential of exosomes in Alzheimer's disease. Journal of Neurochemistry, 156. Blackwell Publishing Ltd; 2021. p. 162–81.
[21] Meng Y, Pople CB, Suppiah S, Llinas M, Huang Y, Sahgal A, et al. MR-guided focused ultrasound liquid biopsy enriches circulating biomarkers in patients with brain tumors. Neuro Oncol 2021;23(10):1789–97.
[22] Deng Z, Wang J, Xiao Y, Li F, Niu L, Liu X, et al. Ultrasound-mediated augmented exosome release from astrocytes alleviates amyloid-β-induced neurotoxicity. Theranostics 2021;11(9):4351–62.
[23] Sheybani ND, Batts AJ, Mathew AS, Andrew Thim E, Price RJ. Focused ultrasound hyperthermia augments release of glioma-derived extracellular vesicles with differential immunomodulatory capacity. Theranostics 2020;10(16):7436–47.
[24] Tang Y, Wu Z, Guo R, Huang J, Rong X, Zhu B, et al. Ultrasound-augmented anti-inflammatory exosomes for targeted therapy in rheumatoid arthritis. J Mater Chem B 2022;10(38):7862–74.
[25] Xia P, Wang Q, Song J, Wang X, Wang X, Lin Q, et al. Low-intensity pulsed ultrasound enhances the efficacy of bone marrow−derived MSCS in osteoarthritis cartilage repair by regulating autophagy-mediated exosome release. Cartilage 2022;13(2):1–13.
[26] Bae S, Liu K, Pouliopoulos AN, Ji R, Jiménez-Gambín S, Yousefian O, et al. Transcranial blood-brain barrier opening in Alzheimer's disease patients using a portable focused ultrasound system with real-time 2-D cavitation mapping. Theranostics 2024;14(11):4519–35.
[27] Catalano M, O'Driscoll L. Inhibiting extracellular vesicles formation and release: a review of EV inhibitors. J Extracell Vesicles 2019;9(1):1–22. doi: 10.1080/20013078.2019.1703244.
[28] Choi JJ, Pernot M, Small SA, Konofagou EE. Noninvasive, transcranial and localized opening of the blood-brain barrier using focused ultrasound in mice. Ultrasound Med Biol 2007;33(1):95–104.
[29] Feshitan JA, Chen CC, Kwan JJ, Borden MA. Microbubble size isolation by differential centrifugation. J Colloid Interface Sci 2009;329(2):316–24.
[30] Wang S, Samiotaki G, Olumolade O, Feshitan JA, Konofagou EE. Microbubble type and distribution dependence of focused ultrasound-induced blood-brain barrier opening. Ultrasound Med Biol 2014;40(1):130–7.
[31] Perneczky R, Wagenpfeil S, Komossa K, Grimmer T, Diehl J, Kurz A. Mapping scores onto stages: mini-mental state examination and clinical dementia rating. Am J Geriatr Psychiatry 2006;14(2):139–44.
[32] Kim J, Lee H, Park K, Shin S. Rapid and efficient isolation of exosomes by clustering and scattering. J Clin Med 2020;9(3):650.
[33] Sun T, Samiotaki G, Wang S, Acosta C, Chen CC, Konofagou EE. Acoustic cavitation-based monitoring of the reversibility and permeability of ultrasound-induced blood-brain barrier opening. Phys Med Biol 2015;60(23):9079–94.
[34] Ji R, Karakatsani ME, Burgess M, Smith M, Murillo MF, Konofagou EE. Cavitation-modulated inflammatory response following focused ultrasound blood-brain barrier opening. J Control Release 2021;337:458–71.
[35] Kovacs ZI, Kim S, Jikaria N, Qureshi F, Milo B, Lewis BK, et al. Disrupting the blood-brain barrier by focused ultrasound induces sterile inflammation. Proc Natl Acad Sci U S A 2017;114(1):E75–84.
[36] Lee S, Mankhong S, Kang JH. Extracellular vesicle as a source of Alzheimer's biomarkers: opportunities and challenges. Int J Mol Sci 2019;20(7):1–23. doi: 10.3390/ijms20071728.
[37] Khan NA, Asim M, El-Menyar A, Biswas KH, Rizoli S, Al-Thani H. The evolving role of extracellular vesicles (exosomes) as biomarkers in traumatic brain injury: Clinical perspectives and therapeutic implications. Front Aging Neurosci 2022;14:1–27.
[38] Laulagnier K, Javalet C, Hemming FJ, Sadoul R. Purification and analysis of exosomes released by mature cortical neurons following synaptic activation. Exosomes and Microvesicles; 2017129–38.
[39] Yuan Q, dong Li X, miao Zhang S, wei Wang H, liang Wang Y. Extracellular vesicles in neurodegenerative diseases: Insights and new perspectives. Genes Dis 2021;8(2):124–32.
[40] Li P, Kaslan M, Lee SH, Yao J, Gao Z. Progress in Exosome Isolation Techniques. Theranostics 2017;7(3):789–804.
[41] Yang Y, Wang Y, Wei S, Zhou C, Yu J, Wang G, et al. Extracellular vesicles isolated by size-exclusion chromatography present suitability for RNomics analysis in plasma. J Transl Med 2021;19(1):1–12.